TURKISH JOURNAL OF
ORTHODONTICS

DOI: 10.4274/TurkJOrthod.2025.2025.21

Original Article

# Three-Dimensional Evaluation of Midfacial Changes After Maxillary Skeletal Expander Application: A Retrospective Study

Fırat Vural, Yeşim Kaya, Özer Alkan

Ankara Yıldırım Beyazıt University Faculty of Dentistry, Department of Orthodontics, Ankara, Türkiye

**Cite this article as:** Vural F, Kaya Y, Alkan Ö. Three-dimensional evaluation of midfacial changes after maxillary skeletal expander application: a retrospective study. *Turk J Orthod.* 2025; 38(4): 190-198



**Main Points**

- The maxillary skeletal expander 2 application resulted in greater skeletal expansion and less dental tipping.
- The coronal zygomatic section exhibited a pyramidal skeletal expansion pattern.
- An axial palatal section showed a parallel split of the midpalatal suture.

## ABSTRACT

**Objective:** This study aimed to investigate the skeletal and dental effects of the maxillary skeletal expander (MSE) using cone beam computed tomography (CBCT) images analyzed in the coronal zygomatic and axial palatal sections (APS).

**Methods:** Pre- and post-expansion CBCT images of 18 subjects (10 females and 8 males) aged 12-16 years with maxillary transverse deficiency who were treated with MSE 2 were included in this retrospective study. In the coronal zygomatic section (CZS), upper interzygomatic distance and lower interzygomatic distances (LID), orbital distance (OD), alveolar distances (AD), and dental distances (DD), as well as nasal cavity width (NCW) and molar basal bone angle, were assessed. In the APS, the separation between the anterior nasal spine (ANS) and posterior nasal spine (PNS) was assessed. All measurements were performed using OnDemand3D software. Pre- and post-expansion treatment changes were compared using paired t-tests, with statistical significance set at $p<0.05$.

**Results:** In the CZS, a pyramidal skeletal expansion pattern was observed, with the greatest increase in DD (R: 2.83 mm, L: 3.18 mm), followed by AD (R: 1.63 mm, L: 1.97 mm), NCW (R: 1.66 mm, L: 2.28 mm), LID (R: 1.48 mm, L: 1.92 mm), and OD (R: 0.42 mm, L: 0.56 mm). Along with greater skeletal expansion, slightly reduced dental tipping and minimal alveolar bone bending were observed. In the APS, a nearly equal separation was observed at both the ANS (R: 1.79 mm, L: 2.46 mm) and PNS (R: 1.85 mm, L: 2.49 mm), indicating a parallel split of the midpalatal suture. Furthermore, among the 36 pterygopalatine sutures examined, only three showed separation between the medial and lateral pterygoid processes.

**Conclusion:** MSE 2 application provides more favorable skeletal outcomes reduces dentoalveolar side effects, and results in a more parallel midpalatal suture split.

**Keywords:** Maxillary skeletal expander, MSE 2, midpalatal suture, cone beam computed tomography

## INTRODUCTION

Maxillary transverse deficiency is a common skeletal anomaly that may present alone or alongside sagittal and vertical discrepancies.[1] Limited visibility of the posterior maxilla often results in a lower treatment demand for isolated transverse deficiency than for sagittal or vertical anomalies.[1,2] Nevertheless, this condition can significantly affect jaw function and facial appearance.[1]

**Corresponding author:** Assoc. Prof. Yeşim Kaya, **e-mail:** yesimkaya82@hotmail.com
**Received:** April 14, 2025 **Accepted:** October 10, 2025 **Publication Date:** 30.12.2025

The midpalatal and transpalatal sutures are the primary intermaxillary growth sites influencing transverse and anteroposterior maxillary development.[3] Orthopedic separation of these sutures using palatal expanders is the primary treatment for maxillary transverse deficiency.[1,3] The morphology of the sutures changes over time: it is broad and V-shaped in the infantile period, wavy in the juvenile period, and more tortuous with increasing interdigitation in the adolescent period.[4] In addition to the increasing resistance over time of the midpalatal and transpalatal sutures, the resistance of the circummaxillary sutures that articulate with the maxilla also affects palatal expander design and activation protocols.[5]

Rapid palatal expansion using conventional tooth-borne appliances that apply heavy orthopedic forces is one treatment option.[6] Although the primary goal is to maximize skeletal effects, dentoalveolar side effects, such as alveolar bone bending and dental tipping, are frequent.[6,7] To minimize these side effects, various mini-screw-assisted rapid palatal expanders (MARPE)-tooth-bone-borne (hybrid) and bone-borne-have been developed.[8]

The skeletal and dentoalveolar effects of MARPE vary according to miniscrew position and whether monocortical or bicortical anchorage is used.[9-11] A more parallel sutural opening can be achieved by inserting bicortically engaged miniscrews as posteriorly and as deeply into the palate as possible.[11-13] The maxillary skeletal expander (MSE), a type of MARPE, achieves bicortical engagement by inserting four miniscrews into the cortical bone of the palate and the nasal floor. These screws are positioned in the posterior maxilla, beneath the zygomatic buttress, adjacent to the midpalatal suture, and at the deepest point of the palate.[12,13] As a purely bone-borne device, the MSE produces more pronounced skeletal changes with minimal dentoalveolar effects.[7,13]

MSE 2, a type of MSE, is an effective non-surgical option for late adolescents and young adults when sutural rigidity is increased.[13] Its clinical utility extends beyond conventional orthodontic expansion, encompassing broader indications, including airway volume enhancement, management of facial asymmetry, and preparation for orthognathic surgery.[14,15] Recent studies have highlighted its capacity to reduce age-dependency and to extend the therapeutic window for skeletal expansion, thereby establishing its distinct role in contemporary orthodontics.[13,16]

Numerous studies have examined the skeletal and dental effects of MSE, using cone-beam computed tomography (CBCT), particularly in the coronal and axial planes.[5,7,10-13,17-21] These studies included subjects spanning wide age ranges, combining growing and non-growing individuals. McMullen et al.[5] found that MSE produced significantly greater skeletal and dental changes in growing patients than in nongrowing patients, highlighting the importance of growth stage in treatment outcomes. Based on these findings, this study investigated the skeletal and dental effects of MSE 2 in subjects aged 12-16 years, a transitional growth period encompassing the pubertal growth spurt, using CBCT to obtain coronal zygomatic and axial palatal sections (APS). By narrowing the age range and targeting this critical developmental window, our study addresses an important gap in the current literature and provides clinically relevant 3D data that may improve the understanding of age-specific skeletal responses to MSE 2 during adolescence. We hypothesized that MSE 2 would produce significant skeletal expansion with minimal dentoalveolar compensation in adolescents aged 12-16 years.

## METHODS

This retrospective study was approved by the Ankara Yıldırım Beyazıt University Ethics Committee of the Health Sciences Institute (approval no: 19/1230, date: 08.12.2022). CBCT images of 18 subjects (10 females, mean age 14.26±1.36 years; 8 males, mean age 14.29±0.72 years; age range: 12-16 years) were selected from the redords of the Department of Oral and Maxillofacial Radiology, Faculty of Dentistry at Ankara Yıldırım Beyazıt University. Baseline orthodontic records indicated that the sample included four normodivergent individuals with mild skeletal Class II malocclusion (ANB: 4.95±0.39°; SN/GoGn: 35.17±1.62°), four normodivergent individuals with mild skeletal Class III malocclusion (ANB: -1.08±0.57°; SN/GoGn: 31.93±4.69°), and ten normodivergent individuals with skeletal Class I relationships (ANB: 1.77±1.22°; SN/GoGn: 31.87±2.12°). Additionally, overjet was increased in 3 individuals (mean 5.13±1.01 mm), was decreased in 4 individuals (mean -0.15±0.60 mm), and was within the ideal range in 11 individuals (mean 2.75±0.70 mm). Furthermore, bilateral posterior crossbite was observed in 14 individuals, while unilateral posterior crossbite was present in 4 individuals. Skeletal maturation assessment of available hand-wrist radiographs revealed that eight individuals were at the MP3cap stage, five at the DP3u stage, and five at the Ru stage. Informed written consent forms, routinely collected at the onset of treatment, included permission to use patient records in scientific research. These forms were signed by each patient and, in the case of those under the age of eighteen, by their parents.

The inclusion criteria were as follows: no previous orthodontic treatment, no systemic disease, and no history of trauma or craniofacial surgery; pre- and post-expansion CBCT images with a broad field of view (FOV) including the anterior cranial base; a maxillomandibular bone width discrepancy of more than 5 mm (corresponding to a total expansion activation between 50 and 90 turns) diagnosed using the maxillomandibular differential index;[22] treatment with the MSE 2 appliance (MSE 2, BioMaterials Korea Inc., Seoul, Korea) as described by Cantarella et al.;[20] and successful separation of the midpalatal suture. Poor-quality CBCT images with movement artifacts were excluded from the study.

Previously published studies demonstrated that the standard deviations (σ) for the split of the anterior and posterior nasal spines (PNS) and for maxillary molar inclinations ranged from 0.9 to 2.913, and from 2.20 to 2.38,10, respectively. Based on these findings, standard deviations of 1.9 for linear measurements and 2.0 for angular measurements were assumed. With a Type I error rate of 0.05, an effect size (d) of 0.9, and a Z value of 1.96, the minimum required sample size was calculated using the formula $n=Z^2\sigma^2/d^2$. The resulting sample sizes were 17.12 (rounded to 17) for linear measurements and 18.97 (rounded to 19) for angular measurements. G*Power software (version 3.1; Heinrich-Heine-University, Düsseldorf, Germany) was used to perform the calculations.

The MSE 2 appliance consisted of two molar bands (3M Unitek, Bradford, England) attached to the maxillary first molars, four mini-screw tubes soldered to the expansion screw, and two soft supporting arms connecting these components (Figure 1). Each tube, measuring 1.8 mm in diameter and 2 mm in length, served as a guide for the insertion of four mini-screws. Mini-screws with a diameter of 1.8 mm and a preferred length of 11-13 mm were used to achieve stable bicortical anchorage. The soft supporting arms stabilized the expansion screw, which was positioned on the hard palate between the zygomatic buttresses during miniscrew insertion.[12,20]



After bands were placed on the maxillary molars, an alginate impression was taken and a plaster model was prepared with the bands in proper positions. The expansion screw was positioned according to the manufacturer's guidelines-centered between the second premolars and second molars, aligned with the nasal septum, and placed close to the palatal mucosa. Two long arms on one side of the screw were spot-welded to the molar bands (Lampert Werktechnik GmbH, PUK 5, Germany). The appliance was fitted intraorally and cemented with glass-ionomer band cement (3M Unitek, Monrovia, CA, USA). Four miniscrews were inserted manually with the provided driver. The recommended expansion rate was 0.5-0.8 mm per day until a diastema was observed; thereafter, 0.25 mm per day was used until adequate expansion was achieved. After completion of the expansion, the MSE 2 appliance was left in place to provide retention for at least three months without activation.[20] A detailed evaluation of the patient files revealed a mean expansion of 64.55 tours (minimum: 50; maximum: 90) and a mean retention duration of 4.16 months (minimum: 3; maximum: 6) in this study.

Pre- and post-expansion CBCT images were acquired at the start of expansion and at the end of retention, respectively. The use of the same 3D imaging device (Promax 3D, Planmeca, Helsinki) and scanning procedures (84 kVp, 6 mAs, 8.5 s exposure time, 0.32-mm voxel, 150×110×80 mm large FOV) was also ensured.

All CBCT images were exported as digital ımaging and communications in medicine files and stored. OnDemand3D software (CyberMed Inc., Seoul, Korea) was used to superimpose the pre- and post-expansion CBCT images , using the anatomical structures of the anterior cranial base as a reference. The superimposition method is based on automated matching of grayscale voxel patterns (Figure 2).

After successfully superimposing the pre- and post-expansion CBCT images using OnDemand3D software, two reference planes were identified. Upper interzygomatic distance (UID), lower interzygomatic distance (LID), orbital distance (OD), alveolar bone distance, and dental distance (DD), nasal cavity width (NCW), and maxillary basal bone angle were measured in the coronal zygomatic section (CZS), which passes through the uppermost point of the frontozygomatic sutures and the lowest point of the zygomaticomaxillary sutures (Figure 3). The separation of the anterior and PNS and the articulation between the pyramidal process of the palatine bone and the pterygoid notch, located between the medial and lateral plates of the pterygoid process, were evaluated in the APS. The APS

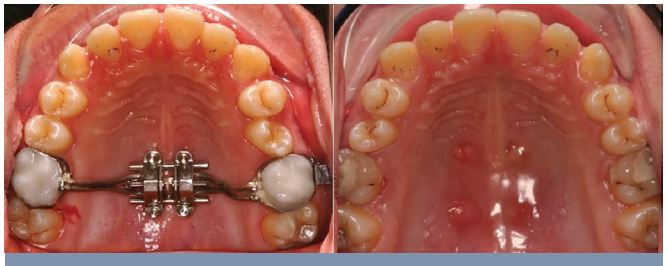

**Figure 1.** Pre- and post-expansion images of the MSE 2 appliance. MSE, maxillary skeletal expander.

**Figure 2.** Pre- and post-expansion superimposed CBCT images. CBCT, cone beam computed tomography.

passes through the anterior and PNS and is perpendicular to the midsagittal plane defined by the anterior nasal spine (ANS), the PNS and the nasion (Figure 4). The skeletal linear and angular measurements used in this study, along with their definitions, are presented in Table 1.

### Statistical Analysis

A maxillofacial radiologist (AA) with over 10 years of experience in CBCT image analysis conducted all skeletal and linear measurements. To evaluate the intra-observer error, eight randomly selected pre- and post-expansion CBCT images were re-superimposed and re-traced four weeks after the initial tracing. To assess the measurement precision, intra-examiner reliability was calculated and found to be high (intraclass correlation coefficient: 0.890; $p<0.001$). Additionally, to assess inter-observer reliability, a second maxillofacial radiologist (BÇ) independently repeated the measurements on the same images and a similarly level of inter-observer agreement was observed (intraclass correlation coefficient: 0.820; $p<0.001$). Random measurement error was calculated using Dahlberg's formula, and it was observed that the error values ranged from 0.14° to 0.19° for the one angular measurement and from 0.032 to 0.046 mm for the eight linear measurements.

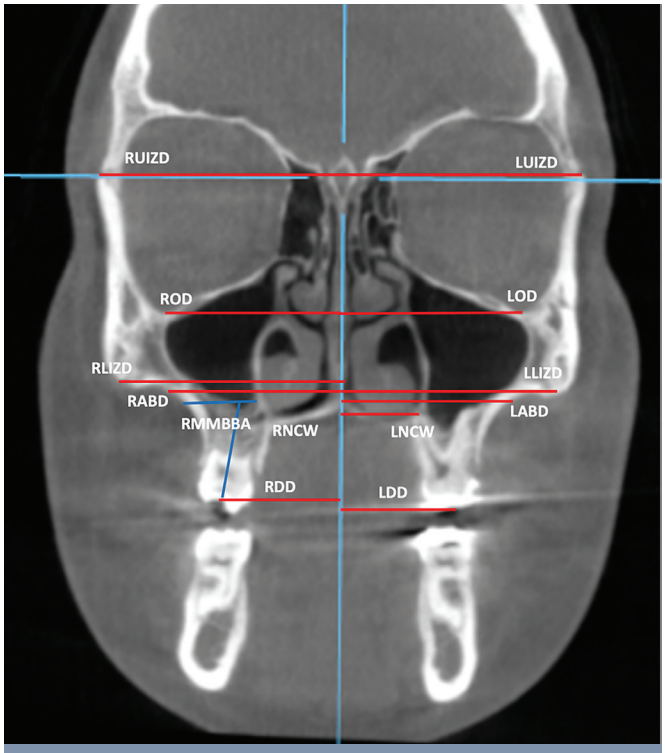


**Figure 3.** Coronal zygomatic section. Red lines represent linear measurements, and blue lines indicate angular measurements.

RUIZD, right upper interzygomatic distance; LUIZD, left upper interzygomatic distance; ROD, right orbital distance; LOD, left orbital distance; RLIZD, right lower interzygomatic distance; LIIZD, left lower interzygomatic distance; RABD, right alveolar bone distance; LABD, left alveolar bone distance; RNCW, right nasal cavity width; LNCW, left nasal cavity width; RDD, right dental distance; LDD, left dental distance; RMMBBA, right maxillary molar basal bone angle; LMMBBA, left maxillary molar basal bone angle.

Descriptive statistics for the continuous variables were presented as means and standard deviations. The normality assumption for the continuous variables was tested using the Kolmogorov-Smirnov test. A paired t-test was used to compare the means of pre- and post-expansion changes, as well as the right and left sides, for normally distributed variables. The statistical significance level was set at 5%, and analyses were performed using SPSS (version 21; Chicago, IL).

## RESULTS

Skeletal linear and angular measurements in the CZS, except for NCW, did not differ significantly between the left and right sides in both pre- and post-expansion CBCT images. The left NCW (2.28 mm) was greater than the right (1.66 mm) (Table 2).

The treatment changes were as follows: 0.40 and 0.67 mm in the UID, 0.42 and 0.56 mm in the OD, 1.48 and 1.92 mm in the LID, 1.66 and 2.28 mm in the NCW, 1.63 and 1.97 mm in the alveolar bone distance, 2.83 and 3.18 mm in the DD, and 3.06 and 2.70° in the molar basal bone angle (MBBA) for the right and left sides, respectively. The increased expansion in the superior-inferior direction confirms the pyramidal pattern of skeletal expansion.



While LID represents pure skeletal expansion, alveolar bone distance represents skeletal expansion combined with alveolar bone bending, and DD represents skeletal expansion combined with alveolar bone bending and dental tipping. Based on this, the amounts of skeletal expansion, alveolar bone bending, and dental tipping for the right and left sides were calculated to be 1.48 and 1.92 mm, 0.15 and 0.05 mm, and 1.20 and 1.21 mm, respectively. These results indicate greater skeletal expansion, slightly less dental tipping, and negligible alveolar bone bending. The increase in the maxillary MBBA also confirms the presence of dental tipping (Table 2).


**Figure 4.** Axial palatal section showing anatomical landmarks.

RANS, right anterior nasal spine; LANS, left anterior nasal spine; RPNS, right posterior nasal spine; LPNS, left posterior nasal spine; R Lat Pter, lateral plate of the right pterygoid process; R Med Pter, medial plate of the right pterygoid process; L Med Pter, medial plate of the left pterygoid process; L Lat Pter, lateral plate of the left pterygoid process.

In the APS, the treatment changes at the anterior and PNSs were 1.79 and 2.46 mm for the right side, and 1.85 and 2.49 mm for the left side.

Because the amounts in the anterior and posterior regions of the maxilla were nearly equal, a parallel split of the midpalatal suture was observed. On the other hand, an asymmetry in the midpalatal suture split was observed, with greater separation on the left than on the right (Table 3). Moreover, only three of the 36 pterygopalatine sutures showed separation between the medial and lateral pterygoid processes.

A consistent asymmetry was observed in several measurements, with greater expansion noted on the left side compared to the right. This was evident in reduced interzygomatic distance (p=0.047), NCW (p=0.001), and ANS separation (p=0.002), as detailed in Tables 2 and 3.

## DISCUSSION

In the CZS, the results of this study demonstrated greater skeletal expansion, slightly less dental tipping, and negligible alveolar bone bending. Moreover, a pyramidal skeletal expansion pattern was determined by the greatest increase in DD, followed by increases in alveolar bone distance, NCW, LID, and OD. In the APS, a parallel split of the midpalatal suture was observed. Based on these findings, our hypothesis was supported.

The reliability of CBCT-based 3D analysis for assessing skeletal and dentoalveolar changes has been confirmed in recent studies.[23,24] CBCT combined with multiplanar reorientation techniques enabled precise landmark localization at a voxel size of 0.32 mm, ensuring high-resolution imaging while maintaining acceptable radiation exposure.[23] Landmark

**Table 1.** Skeletal linear and angular mesurements investigated in the coronal zygomatic and axial palatal sections

| | Measurements | Definitions |
|---|---|---|
| Coronal zygomatic section | **Right upper interzygomatic distance** | Distance of the outermost point of the right frontozygomatic suture to the midsagittal plane |
| | **Left upper interzygomatic distance** | Distance of the outermost point of the left frontozygomatic suture to the midsagittal plane |
| | **Right orbital distance** | Distance of the lowest point on the right inferior orbital margin to the midsagittal plane |
| | **Left orbital distance** | Distance of the lowest point on the left inferior orbital margin to the midsagittal plane |
| | **Right lower interzygomatic distance** | Distance of the outermost point of the right zygomaticomaxillary suture to the midsagittal plane |
| | **Left lower interzygomatic distance** | Distance of the outermost point of the left zygomaticomaxillary suture to the midsagittal plane |
| | **Right alveolar bone distance** | Distance of the alveolar bone point at the level of the apical of the maxillary right first molar root to the midsagittal plane |
| | **Left alveolar bone distance** | Distance of the alveolar bone point at the level of the apical of the maxillary left first molar root to the midsagittal plane |
| | **Right nasal cavity width** | Distance of the most anterior portion of the inferior contour of the right nasal cavity to the midsagittal plane |
| | **Left nasal cavity width** | Distance of the most anterior portion of the inferior contour of the left nasal cavity to the midsagittal plane |
| | **Right dental distance** | Distance of the occlusal contact point located at the central fossa of the right maxillary first molar to the midsagittal plane |
| | **Left dental distance** | Distance of the occlusal contact point located at the central fossa of the left maxillary first molar to the midsagittal plane |
| | **Right maxillary molar basal bone angle** | The angle formed between the line connecting the most lateral point of the right maxillary bone and the merge point of cortical bones of the nasal floor and maxillary sinus, and the line connecting the central pit of the right maxillary first molar crown to the furcation of the roots |
| | **Left maxillary molar basal bone angle** | The angle formed between the line connecting the most lateral point of the left maxillary bone and the merge point of cortical bones of the nasal floor and maxillary sinus, and the line connecting the central pit of the left maxillary first molar crown to the furcation of the roots |
| Axial palatal section | **Right anterior nasal spine** | Distance of the right anterior nasal spine to the midsagittal plane |
| | **Left anterior nasal spine** | Distance of the left anterior nasal spine to the midsagittal plane |
| | **Right posterior nasal spine** | Distance of the right posterior nasal spine to the midsagittal plane |
| | **Left posterior nasal spine** | Distance of the left posterior nasal spine to the midsagittal plane |
| | **Right lateral-medial pterygoid process** | The split of the right lateral and medial pterygoid process |
| | **Left lateral-medial pterygoid process** | The split of the left lateral and medial pterygoid process |

identification was performed by calibrated observers, showing high intra- and inter-observer agreement. These findings are consistent with previous literature supporting the reproducibility and diagnostic accuracy of CBCT-based measurements in orthodontics.[23,24]

In light of the observed skeletal changes, our findings should be interpreted within the context of existing expansion-based orthopedic protocols. Previous studies, particularly those involving alternating expansion and constriction, have demonstrated that such approaches effectively disarticulate the circummaxillary sutures and facilitate maxillary displacement.[25,26] Despite variations in appliance design and treatment timing, these protocols share a common biomechanical principle whereby sutural loosening enhances the orthopedic response to protraction forces. In line with this rationale, the present results obtained with the MSE 2 appliance confirm that transverse expansion can induce clinically meaningful skeletal changes in adolescents, likely by operating through sutural disarticulation mechanisms similar to those described in previous protocols.

Since the treatment changes may vary depending on the location of the miniscrew and the design of the appliance,



**Table 2.** Skeletal angular and linear measurements investigated in the coronal zygomatic section

| | | Pre-expansion (Mean±SD) | Post-expansion (Mean±SD) | Treatment change (Mean±SD) | p |
|---|---|---|---|---|---|
| Upper interzygomatic distance | **Right** | 50.13±2.55 | 50.54±2.55 | 0.40±0.36 | 0.001 |
| | **Left** | 50.18±2.43 | 50.86±2.49 | 0.67±0.54 | 0.001 |
| | **p** | 0.809 | 0.141 | | |
| Orbital distance | **Right** | 30.52±1.96 | 30.94±1.96 | 0.42±1.96 | 0.001 |
| | **Left** | 30.87±2.09 | 31.43±2.18 | 0.56±2.13 | 0.001 |
| | **p** | 0.410 | 0.289 | | |
| Lower interzygomatic distance | **Right** | 43.53±2.53 | 45.01±2.62 | 1.48±1.20 | 0.001 |
| | **Left** | 43.79±3.02 | 45.72±2.85 | 1.92±0.88 | 0.001 |
| | **p** | 0.422 | 0.047 | | |
| Nasal cavity width | **Right** | 12.97±1.73 | 14.63±2.01 | 1.66±1.87 | 0.001 |
| | **Left** | 14.02±1.51 | 16.30±1.89 | 2.28±1.7 | 0.001 |
| | **p** | 0.001 | 0.001 | | |
| Alveolar bone distance | **Right** | 29.83±1.85 | 31.46±1.83 | 1.63±1.33 | 0.001 |
| | **Left** | 30.22±2.51 | 32.20±2.60 | 1.97±1.41 | 0.001 |
| | **p** | 0.337 | 0.139 | | |
| Dental distance | **Right** | 22.46±1.54 | 25.30±1.50 | 2.83±1.52 | 0.001 |
| | **Left** | 22.61±2.59 | 25.80±1.90 | 3.18±1.49 | 0.001 |
| | **p** | 0.789 | 0.250 | | |
| Maxillary molar basal bone angle | **Right** | 90.40±6.83 | 93.47±5.46 | 3.06±2.67 | 0.001 |
| | **Left** | 92.07±4.85 | 94.78±3.50 | 2.70±2.08 | 0.001 |
| | **p** | 0.319 | 0.322 | | |

p<0.05, Paired t-test was perfomed.
SD, standard deviation.

**Table 3.** Skeletal linear measurements investigated in the axial palatal section

| | | Pre-expansion (Mean±SD) | Post-expansion (Mean±SD) | Treatment change (Mean±SD) | p |
|---|---|---|---|---|---|
| Anterior nasal spine | **Right** | - | 1.79±0.69 | 1.79±0.69 | 0.001 |
| | **Left** | - | 2.46±0.89 | 2.46±0.89 | 0.001 |
| | **p** | - | 0.002 | | |
| Posterior nasal spine | **Right** | - | 1.85±0.67 | 1.85±0.67 | 0.001 |
| | **Left** | - | 2.49±0.85 | 2.49±0.85 | 0.001 |
| | **p** | - | 0.003 | | |

p<0.05, Paired t-test was perfomed.
SD, standard deviation.

the skeletal expansion patterns produced by different MSEs have been examined in many previous studies.[5,10,11,18-20,27] Among those studies using CZSs from CBCT images, Chun et al.[28] investigated a tooth-bone-borne MARPE appliance that included four miniscrews inserted medial to the first premolars and distal to the first molars. A sequential increase in transverse measurements was reported from the upper interzygomatic region to the dental arch, reflecting a pyramidal skeletal expansion pattern with the apex near the frontonasal area and the base at the dentoalveolar level.[28]

Moon et al.[10] compared tooth-bone-borne (MSE 2) and tissue-bone-borne (C-Expander) appliances and reported comparable increases in maxillary and dental widths. In another study,[11] MSE 2 was compared with bone-borne expanders in which two miniscrews were inserted in the anterior palate at the level of the third rugae, and two were placed between the second premolar and the first molar. Both groups demonstrated similar increases in the lower interzygomatic and intermolar distances; however, the bone-borne group showed greater increases in OD and NCW.[11] Collectively, these studies indicate that MSE 2 and bone-borne expanders yield nearly identical skeletal effects, with MSE 2 potentially preferable in clinical situations requiring efficient skeletal expansion with less impact on the upper midface.



Among studies that specifically investigated MSE2 expanders, Cantarella et al.,[20] Paredes et al.,[7] McMullen et al.,[5] and Tang et al.[19] consistently reported significant skeletal and dentoalveolar changes, including increases in interzygomatic, alveolar, intermolar, and nasal cavity dimensions. The treatment changes observed in our study were generally in line with these findings, with minor differences likely related to variations in age ranges and in the total amount of expansion among study groups.[5,7,10,11,19,20]

Furthermore, the pyramidal skeletal expansion pattern observed in our sample, characterized by progressive displacement from the orbital and zygomatic regions toward the dentoalveolar level, was consistent with the expansion gradient described in prior MSE-based research.[5,11,19] Similarly, Ding et al.[16] demonstrated that MSE 2 appliances produce stable long-term skeletal and dentoalveolar expansion, with preservation of the pyramidal expansion pattern even after the retention phase. This consistent pattern across studies highlights the reliable biomechanical effect of the MSE 2 appliance and its potential predictability for clinical planning.

Tipping of the anchor teeth is a common side effect of MSE 2 expanders, because the gap between the miniscrews and their surrounding holes results in the anchor teeth being loaded primarily during initial activation.[5] In the present study, a significant amount of dental tipping was observed consistent with the study results of Paredes et al.[7] and Moon et al.[10] On contrary, our maxillary MBBA results, which confirms the dental tipping, generally agreed with the studies of Moon et al.[10] and Cantarella et al.[20] while lower than Paredes et al.[7] study. We also determined lower alveolar bone bending results compared to Paredes et al.[7] study. The discrepancy observed in dental tipping and alveolar bone bending between Paredes et al.[7] results and ours might result from the measurement method and age range of the study groups, respectively. Taken together, these findings emphasize the need to monitor early tipping forces carefully during MSE 2 treatment, particularly in growing patients. Moreover, recent reports indicate that maxillary transverse discrepancies should also be assessed in relation to molar rotations[29] and by employing different CBCT-based diagnostic methods that account for skeletal patterns,[30] as these factors may further influence treatment outcomes and long-term stability.

Most recently, Elawady et al.[31] conducted a randomized controlled trial using CBCT in young adults to evaluate MSE with and without micro-osteoperforations (MOP). They reported that MOP-assisted MSE resulted in significantly greater increases in nasal cavity and interzygomatic widths compared with standard MSE, whereas dental tipping and alveolar bending were comparable between groups.[31] These findings suggest that MOP can enhance the skeletal efficiency of expansion without causing dental side effects, complementing our results and providing practical insights into adjunctive techniques that may optimize treatment outcomes.

Previous studies have shown that during maxillary expansion, the inferior part of the pterygoid process tends to displace laterally with the hemimaxillae, whereas the superior part remains largely stable.[18,32] Age-related increases in sutural interdigitation have also been reported to make disarticulation of the palatal bone from the pterygoid process more difficult, thereby influencing the overall expansion pattern.[12,33] Despite these limitations, several MSE studies have demonstrated a parallel midpalatal suture split.[5,12,13,18] In the present study, we likewise observed a parallel split, with a nearly equal separation between the anterior and posterior regions of the maxilla. However, of the 36 pterygopalatine sutures examined, only three showed separation between the medial and lateral pterygoid processes.

Notably, an asymmetrical expansion pattern was detected, with greater skeletal and dental changes on the left side. This left-dominant expansion may reflect underlying anatomical asymmetries, variations in screw placement, or differences in initial molar inclination. Similar asymmetry has been noted in previous studies of MSE and MARPE appliances, which have reported unequal expansion patterns potentially associated with morphological differences in the maxilla, asymmetry in bone density, or uneven force distribution during screw activation.[21,27]

In contrast to prior studies that included broad age ranges, the present study focused solely on adolescents, allowing for a more controlled assessment of skeletal and dentoalveolar changes associated with MSE 2. This targeted approach enhances the interpretability of expansion outcomes in growing patients and helps establish a consistent reference point for future

clinical and radiographic research. By integrating multiplanar CBCT analysis with age-specific evaluation, the study addresses a notable gap in the literature regarding the skeletal effects of MSE 2 during adolescence. Furthermore, the demonstrated ability of MSE 2 to achieve significant skeletal expansion with minimal dentoalveolar side effects, particularly for borderline surgical cases, reinforces its clinical utility and supports its value in treatment planning and growth-phase-specific decision-making.

### Study Limitations

The main limitations of this study included its retrospective design, relatively small sample size, mixed sample of male and female participants, limited age range, and short follow-up periods. It is therefore recommended that future studies be designed as prospective, randomized trials involving both males and females across various age groups, with standardized appliance activation protocols, controlled operator variability, and long-term follow-up periods, including CBCT scans at least one year post-expansion, to further validate and generalize the findings. Additionally, the absence of an untreated control group or of a matched cohort treated with conventional RPE or other MARPE designs limits the ability to assess the relative efficacy of MSE 2. Future research should aim to incorporate well-matched comparative groups to enable a more comprehensive evaluation of different maxillary expansion protocols.

Despite these limitations, the use of CBCT-based three-dimensional imaging enabled high-resolution evaluation of skeletal and dentoalveolar structures, enhancing both the precision and reproducibility of the measurements. Additionally, the inclusion of both coronal and axial evaluation planes contributed to a more comprehensive and spatially accurate analysis.

## CONCLUSION

A pyramidal skeletal expansion pattern was observed in the coronal section of the zygoma. Expansion resulted in greater skeletal displacement, slightly reduced dental tipping, and negligible alveolar bending. A parallel split of the midpalatal suture was observed in the APS. Collectively, these findings support MSE 2 as a favorable treatment option for patients nearing the end of their growth period, producing predominantly skeletal expansion with limited dentoalveolar side effects.

### Ethics

**Ethics Committee Approval:** This retrospective study was approved by the of Ankara Yıldırım Beyazıt University Ethics Committee of the Health Sciences Institute (approval no: 19/1230, date: 08.12.2022).

**Informed Consent:** Written and informed consents were previously signed by the participants or a legal guardian for those under 18 years old.

### Footnotes

**Author Contributions:** Surgicial and Medical Practices - F.V., Y.K.; Concept - Y.K.; Design - Y.K.; Data Collection and/or Processing - F.V., Y.K.; Analysis and/or Interpretation - Y.K., Ö.A.; Literature Search - F.V., Y.K., Ö.A.; Writing - F.V., Y.K.

**Conflict of Interest:** The authors have no conflicts of interest to declare.

**Financial Disclosure:** The authors declared that this study received no financial support.

## REFERENCES

1. Bin Dakhil N, Bin Salamah F. The diagnosis methods and management modalities of maxillary transverse discrepancy. *Cureus.* 2021;13(12):e20482. [CrossRef]
2. Reyneke JP, Conley RS. Surgical/orthodontic correction of transverse maxillary discrepancies. *Oral Maxillofac Surg Clin North Am.* 2020;32(1):53-69. [CrossRef]
3. Carlson DS, Buschang PH. Craniofacial growth and development: evidence-based perspectives. In: Graber LW, ed. Orthodontics: Current principles and techniques. 5th ed. Elsevier, PA: Mosby, 2011:215-246. [CrossRef]
4. Festa F, Festa M, Medori S, et al. Midpalatal suture maturation in relation to age, sex, and facial skeletal growth patterns: a CBCT study. *Children (Basel).* 2024;11(8):1013. [CrossRef]
5. McMullen C, Al Turkestani NN, Ruellas ACO, et al. Three-dimensional evaluation of skeletal and dental effects of treatment with maxillary skeletal expansion. *Am J Orthod Dentofacial Orthop.* 2022;161(5):666-678. [CrossRef]
6. Jia H, Zhuang L, Zhang N, Bian Y, Li S. Comparison of skeletal maxillary transverse deficiency treated by microimplant-assisted rapid palatal expansion and tooth-borne expansion during the post-pubertal growth spurt stage. *Angle Orthod.* 2021;91(1):36-45. [CrossRef]
7. Paredes N, Colak O, Sfogliano L, et al. Differential assessment of skeletal, alveolar, and dental components induced by microimplant-supported midfacial skeletal expander (MSE), utilizing novel angular measurements from the fulcrum. *Prog Orthod.* 2020;21(1):18. [CrossRef]
8. Lin L, Ahn HW, Kim SJ, Moon SC, Kim SH, Nelson G. Tooth-borne vs bone-borne rapid maxillary expanders in late adolescence. *Angle Orthod.* 2015;85(2):253-262. [CrossRef]
9. Li N, Sun W, Li Q, Dong W, Martin D, Guo J. Skeletal effects of monocortical and bicortical mini-implant anchorage on maxillary expansion using cone-beam computed tomography in young adults. *Am J Orthod Dentofacial Orthop.* 2020;157(5):651-661. [CrossRef]
10. Moon HW, Kim MJ, Ahn HW, et al. Molar inclination and surrounding alveolar bone change relative to the design of bone-borne maxillary expanders: a CBCT study. *Angle Orthod.* 2020;90(1):13-22. [CrossRef]
11. Bazzani M, Cevidanes LHS, Al Turkestani NN, et al. Three-dimensional comparison of bone-borne and tooth-bone-borne maxillary expansion in young adults with maxillary skeletal deficiency. *Orthod Craniofac Res.* 2023;26(2):151-162. [CrossRef]
12. Colak O, Paredes NA, Elkenawy I, et al. Tomographic assessment of palatal suture opening pattern and pterygopalatine suture disarticulation in the axial plane after midfacial skeletal expansion. *Prog Orthod.* 2020;21(1):21. [CrossRef]
13. Cantarella D, Dominguez-Mompell R, Mallya SM, et al. Changes in the midpalatal and pterygopalatine sutures induced by micro-

implant-supported skeletal expander, analyzed with a novel 3D method based on CBCT imaging. *Prog Orthod.* 2017;18(1):34. [CrossRef]

14. Moon W. Class III treatment by combining facemask (FM) and maxillary skeletal expander (MSE). *Seminars in Orthodontics.* 2018;24(1):95-107. [CrossRef]
15. Combs A, Paredes N, Dominguez-Mompell R, et al. Long-term effects of maxillary skeletal expander treatment on functional breathing. *Korean J Orthod.* 2024;54(1):59-68. [CrossRef]
16. Ding C, Paredes N, Wu B, Moon W. Long term skeletal, alveolar, and dental expansion effects of the midfacial skeletal expander. *Applied Sciences.* 2023;13(17):9569. [CrossRef]
17. Lee DW, Park JH, Moon W, Seo HY, Chae JM. Effects of bicortical anchorage on pterygopalatine suture opening with microimplant-assisted maxillary skeletal expansion. *Am J Orthod Dentofacial Orthop.* 2021;159(4):502-511. [CrossRef]
18. Song KT, Park JH, Moon W, Chae JM, Kang KH. Three-dimensional changes of the zygomaticomaxillary complex after mini-implant assisted rapid maxillary expansion. *Am J Orthod Dentofacial Orthop.* 2019;156(5):653-662. [CrossRef]
19. Tang H, Liu P, Liu X, et al. Skeletal width changes after mini-implant-assisted rapid maxillary expansion (MARME) in young adults. *Angle Orthod.* 2021;91(3):301-306. [CrossRef]
20. Cantarella D, Dominguez-Mompell R, Moschik C, et al. Midfacial changes in the coronal plane induced by microimplant-supported skeletal expander, studied with cone-beam computed tomography images. *Am J Orthod Dentofacial Orthop.* 2018;154(3):337-345. [CrossRef]
21. Cantarella D, Dominguez-Mompell R, Moschik C, et al. Zygomaticomaxillary modifications in the horizontal plane induced by micro-implant-supported skeletal expander, analyzed with CBCT images. *Prog Orthod.* 2018;19(1):41. [CrossRef]
22. Ye G, Li Q, Guo Z, et al. Comparative evaluation of transverse width indices for diagnosing maxillary transverse deficiency. *BMC Oral Health.* 2024;24(1):808. [CrossRef]
23. Lisboa Cde O, Masterson D, da Motta AF, Motta AT. Reliability and reproducibility of three-dimensional cephalometric landmarks using CBCT: a systematic review. *J Appl Oral Sci.* 2015;23(2):112-119. [CrossRef]
24. Gribel BF, Gribel MN, Frazão DC, McNamara JA Jr, Manzi FR. Accuracy and reliability of craniometric measurements on lateral cephalometry and 3D measurements on CBCT scans. *Angle Orthod.* 2011;81(1):26-35. [CrossRef]
25. Liou EJ, Tsai WC. A new protocol for maxillary protraction in cleft patients: repetitive weekly protocol of alternate rapid maxillary expansions and constrictions. *Cleft Palate Craniofac J.* 2005;42(2):121-127. [CrossRef]
26. Borzabadi-Farahani A, Lane CJ, Yen SL. Late maxillary protraction in patients with unilateral cleft lip and palate: a retrospective study. *Cleft Palate Craniofac J.* 2014;51(1):e1-e10. [CrossRef]
27. Park JJ, Park YC, Lee KJ, Cha JY, Tahk JH, Choi YJ. Skeletal and dentoalveolar changes after miniscrew-assisted rapid palatal expansion in young adults: a cone-beam computed tomography study. *Korean J Orthod.* 2017;47(2):77-86. [CrossRef]
28. Chun JH, de Castro ACR, Oh S, et al. Skeletal and alveolar changes in conventional rapid palatal expansion (RPE) and miniscrew-assisted RPE (MARPE): a prospective randomized clinical trial using low-dose CBCT. *BMC Oral Health.* 2022;22(1):114. [CrossRef]
29. Özden S, Cicek O. Analysis of the effect of maxillary transverse deficiencies on permanent maxillary first molar rotations using 3D digital models. *BMC Oral Health.* 2025;25(1):879. [CrossRef]
30. Chen Z, Guo R, Qin Q, Feng J, Zheng Y, Li W. Transverse analysis of maxillary transverse deficiency and sagittal skeletal patterns: a cone-beam computed tomography study. *Am J Orthod Dentofacial Orthop.* 2025;168(3):317-326.e3. [CrossRef]
31. Elawady AR, Abd Alfatah EB, Mohamed RE, Hussein FA, Ali MM, Shendy MA. Evaluation of maxillary skeletal expander (MSE) assisted by two techniques of microoste operforations in young adults using CBCT, a randomised controlled trial. Afr J Bio Sc. 2024;6(7):4192-4206. [CrossRef]
32. Jafari A, Shetty KS, Kumar M. Study of stress distribution and displacement of various craniofacial structures following application of transverse orthopedic forces--a three-dimensional FEM study. *Angle Orthod.* 2003;73(1):12-20. [CrossRef]
33. Savoldi F, Wong KK, Yeung AWK, Tsoi JKH, Gu M, Bornstein MM. Midpalatal suture maturation staging using cone beam computed tomography in patients aged between 9 to 21 years. *Sci Rep.* 2022;12(1):4318. [CrossRef]